

A NEW APPROACH FOR THE FRONT SIDE METALLIZATION OF INDUSTRIAL TYPE SILICON SOLAR CELLS USING A STRUCTURIZATION BY ETCHING

M. Bähr, S. Kim¹, S. Sridharan¹, C. Khadilkar¹, A. Shaikh¹, I. Köhler², M. Reichardt, M. Kumar
SolarZentrum Erfurt, CiS Institut für Mikrosensorik GmbH, Konrad-Zuse-Straße 14,
99099 Erfurt, Germany

¹Ferro Corporation, 1395 Aspen Way, 92083 Vista (CA), USA

²Merck KGaA, Frankfurter Straße 250, 64293 Darmstadt, Germany
Mario Bähr: Tel: +49361-663-1214, Fax: +49361-663-1413, mbaehr@cismst.de

ABSTRACT: This paper investigates the contact formation between silver thick-film paste and silicon on the solar-cell front side. The research was conducted by first opening up a certain area of the SiN_x-anti-reflection coating (ARC) and by then printing silver thick-film contact paste onto silicon directly. To open up the ARC, an etching paste with a certain amount of phosphoric acid was screen printed using a conventional screen printing process. The opening pattern corresponds to the metallization pattern, containing a thin finger grid and busbars. Hence, the metal does no longer need to penetrate the ARC. Therefore, the metal paste formulation can be newly optimized to achieve better contact performance. We focused on the optimization of the contact resistance, using different pastes. Also lead-free pastes were investigated. The manufactured test samples were investigated with regard to the electrical performance of solar cells, the contact resistance between metal and Si, and the observation of silver island growth as an indication for contact formation.

Keywords: Contact formation, metallization, selective etching

1 INTRODUCTION

Most of the industrial type crystalline silicon solar cells are fabricated with silicon nitride ARC on the front side to maximize sunlight absorption. As the next step in industrial processing, silver-thick-film contact paste is then screen printed on the ARC and forms a contact with the emitter after reacting with the ARC during contact firing. Profound analyses were made in order to understand the contact formation process during this firing process¹. It was found that metal oxides – namely glass frits – are playing a major role in the contact formation process.

First there is a reaction of the oxides with the ARC to open up the path for silver to make contact with silicon. Second the glass frits are acting as a buffer to prevent silver from migrating too deeply into the p-n junction. Kontermann reported that some of the SiN_x from the ARC still covers the silicon beneath the metal contact due to the incomplete dissolution of SiN_x². Hence, the effective contact area underneath the metallization is smaller than the metal area that covers the solar cell surface. This effect causes additional shadow loss and can be avoided by means of our approach.

Further, the contact area determines the absolute contact resistance of the metal-semiconductor interface. Remaining SiN_x on the surface increases the contact resistance and limits the fill factor and thus also the conversion efficiency of the solar cell.

Using the cell concept of the present paper, it is possible to predefine the contact area by the separate etching process. So, it is possible to choose the necessary finger width with respect to the minimal contact resistance. However, this finger width will be smaller than typical printed finger width of the firing-through-ARC process, since no remaining ARC is limiting the contact area. Thus, the finger width can be reduced to about 75 % without increasing the contact resistance. A further advantage of the etching process is that unnecessarily large contact areas can be down sized

and detrimental effects on the high surface recombination velocity underneath metal contacts can be reduced. This advantage can be applied to the busbar metallization, where only a metal area to further contact ribbons is necessary, but no contact to the silicon.

To fully transfer these technical gains to high conversion efficiencies, it is, further more, necessary to achieve a low line resistance of the finger metallization. That means a high aspect ratio of the printed fingers and tempts the authors to prefer hotmelt front side metallization pastes³, although this has to be taken as a next step beyond this paper.

Additional, this approach allows us to investigate heavy-metal-free pastes that meet the restriction of the use of hazardous substances (RoHS). For such heavy-metal-free pastes the industrial applicability was already demonstrated.⁴

2 EXPERIMENTAL

The experiments were conducted on typical industrial type Si-solar cells of cell size 72 × 72 mm² and 200 μm thickness. The phosphorus emitter has a sheet resistance of about 50 Ω/sq.. The SiN_x ARC was deposited using PECVD techniques, with a thickness of about 80 nm. For the rear side metallization, a screen printed aluminum paste was applied, to achieve a Al-back-surface field after a cofiring process in an industrial type IR-belt furnace simultaneously to the front side metallization. After firing, the edges of the cells were broken off after laser scribing.

2.1 Local structuring of ARC

To locally remove the SiN_x-ARC layer for contact area opening, the screen printable etching paste *isishape Solar EtchTM BEM* provided by Merck was used. This paste is an already industrialised product whereby the etching process is provided by a certain content of

phosphoric acid. The paste works for both, SiN_x or SiO_2 coatings. The following sketch (Fig. 1) shows a typical processing sequence.

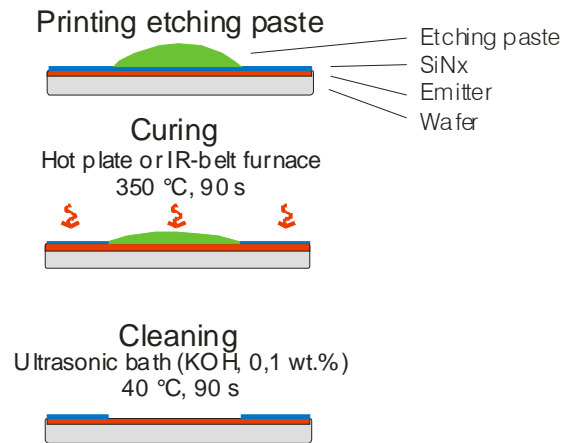


Fig. 1: Process sequence selective structuring of dielectric layers with a screen printable etching paste. Arbitrary structures can be printed, including the typical metallization pattern with busbars and contact fingers.

The paste can be printed using a standard screen-printing-metallization set up usually applied for PV applications, for example cloths with a 280-325 mesh number. After printing, the activation of the paste has to be done by a curing process. This process is necessary since otherwise the paste is not effective. It has to be noticed, that the duration between printing and curing should be rather short (<15 s), otherwise a sloping occurs which enlarges the printed structures.

The curing can be performed at a temperature of 300 – 400°C for about 90 s in an ambient atmosphere. For the process either a hot plate or an infra-red belt furnace can be used. After performing the curing, the sample needs to be cleaned in a 40°C warm ultrasonic bath of KOH (0,1 wt.%). Since all techniques are common in PV industry, this process sequence is ready to be scaled up for industrial processing. A picture with an opened SiN_x coating is shown in Fig. 2. The ARC is removed properly without remaining coating.

Using this process, an opening of dielectric ARC layer can be achieved without damaging the surface underneath. Here, we like to refer to a paper which is also to be presented at this conference⁵. In the experiments carried out, minimal structure width of 85 μm were achieved on texturized or structured surfaces, about 50 μm on non-texturized or flat surfaces. For further experiments, with a 70 μm finger width in the screen a structured finger width of 85 μm was a achieved (70 μm /85 μm), further 85 μm /105 μm and 100 μm /120 μm .

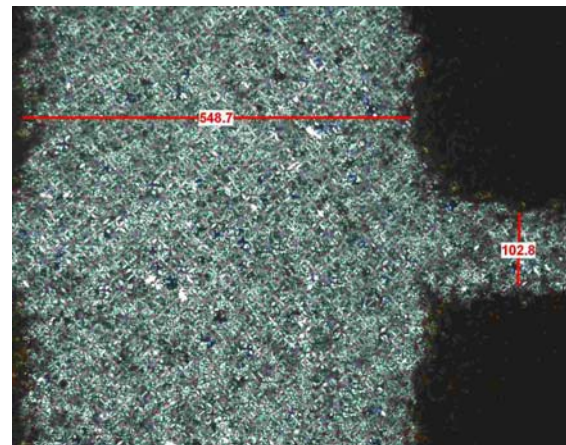


Fig. 2: Optical micrograph of a metallization structure opened using the etching paste. The surface is textured and had been coated with SiN_x . This picture demonstrates the successful removal of the SiN_x layer to determine further contact areas.

2.2 Metallization process

The metallization of front side phosphorus emitter in the previously structured areas was performed by means of screen printing. As explained, the paste compositions were optimized for optimal contact formation to the industrial type phosphorous emitter. To this end, several pastes were composited by Ferro differing in their glass frit contents. The glass frit is responsible for firing through and for the contacting process, thus it is defining the aggressiveness of the formation process. Next to typical lead containing pastes also pastes without heavy metals as lead and cadmium were tested, which meet RoHS.

To investigate the contact formation and further the contact resistance test samples with differently etched structure width for fingers were processed. The etched width was in the same range or even smaller than the width of the printed metal finger. So, the contact area was predefined by etching. In Fig. 3 and Fig. 4 a sketch of both screen printing patterns is shown.

After a screening of several pastes, besides a reference 3 promising pastes were further used for optimizing the processing, further named REF, Paste A, B and C. Pastes REF and A contain lead, the others do not.

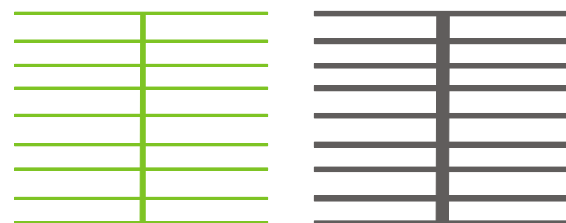


Fig. 3: Draft of the pattern for etching (left) and metallization (right). For the etching pattern, the busbar width is reduced to 0,5 mm, finger width is variable, but always smaller than metallization fingers. For the metallization, the busbar is 1,5 mm wide and the finger width remains constant with nominal 100 μm .

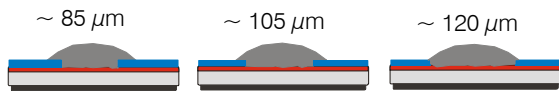


Fig. 4: Sketch of differently etched structure widths for precise determination of the contact area underneath the finger metallization.

The firing is the most crucial process step for the investigated structures. For each paste an optimization was performed, varying the peak temperature and belt speed, what is inverse proportional to the heating time.

3 RESULTS AND DISCUSSION

3.1 Solar cell results

The processed solar cell structures were characterized by means of I-V measurements under standard test conditions (STC). Thereby, the series resistance was determined using two different illumination levels following IEC891.

In Fig. 5 the results are summarized. As one can see, clear trends are visible for the different pastes. Further, V_{OC} and also FF are strongly decreasing for increasing structure width. In general better results were achieved for smallest structure widths. Comparable V_{OC} values to the reference process (without pre-etching) were obtained for the cells printed with paste B and C (both heavy metal free) for the 85 μm structure width. Cells printed with

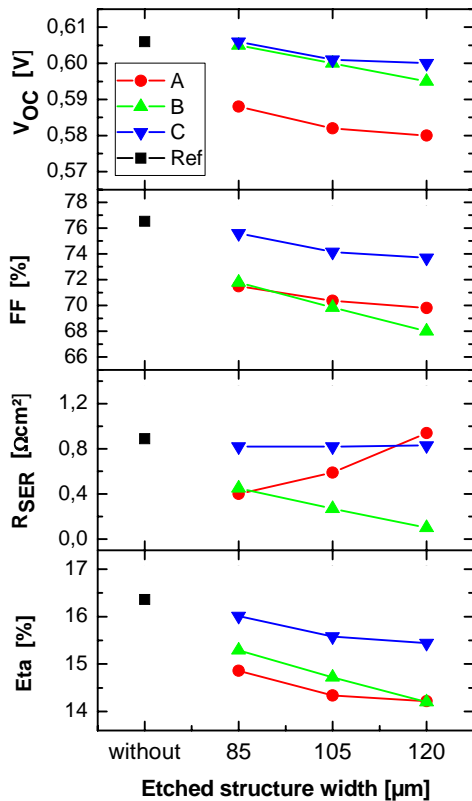


Fig. 5: Electrical properties of processed solar cells with different locally opened finger structures, thus different contact areas. Different symbols refer to different metallization pastes.

paste A (leaded paste) show a significantly lower performance in V_{OC} (loss of about 15 mV). This can be explained by a lower firing temperature of paste REF, which lowers the rear side passivation quality.

Losses in FF for increasing structure width are not directly linked to the resistances (R_{SHUNT} is not shown since the all the values were better than 4 $\text{k}\Omega\text{cm}^2$ and thus not limiting the FF). The series resistance R_{SER} shows for the cells with etched structures different trends: For the cells processed with paste A an increase is observed, whereas, for paste B R_{SER} decreases and, for paste C R_{SER} remains constant. These effects are not fully understood, yet. Still, very low series resistances in the range $<0,6 \Omega\text{cm}^2$ can be achieved, while for the reference cells the typical value is 0,85 Ωcm^2 .

Further more for paste B both, the FF and R_{SER} is decreasing significantly with increasing structure width.

The efficiencies achieved, were for the best cells with pre-etching and using lead free metal paste C, in the range of 16 %. When compared to the reference cell with about 16,5 %, those cells suffer from a slightly decreased FF .

In conclusion, the presented process scheme is best suited for lead-free pastes, since these pastes fir better to the thermal requirements of the cofiring process, and thus rear side passivation making use of an Al-BSF, than the lead containing paste.

3.2 Contact resistance measurements

Specific contact resistance $R_{C,S}$ between the metallization and silicon (emitter) was measured using the transfer length method (TLM): A 4-point measurement is performed between finger structures with a certain distance (Fig. 6) on a typically processed wafer (see Experimental, section 2). By increasing the distance between two structures, the resistance increases. The measured resistance consists of contact resistance that contributes to all measurements in the same way and of the sheet resistance which is depending on the distances. Thus, both contributions can be calculated independently from the dataset.

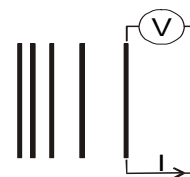


Fig. 6: TLM structure. The resistance between neighbouring finger structures is measured to determine both, the specific contact resistance $R_{C,S}$ and the sheet resistance R_S .

In Fig. 7 the results are shown. One would expect a constant resistance with increasing contact area (cf. R_{SER} in section 3.1). But for all pastes investigated which were combined with a pre-etching process, an increase is observed. For the samples processed with pre-etching and lead-and cadmium-free paste B specific contact resistances nearly one magnitude lower compared to the standard firing through paste (0,07 vs. 0,56 $\text{m}\Omega\text{cm}^2$) was obtained.

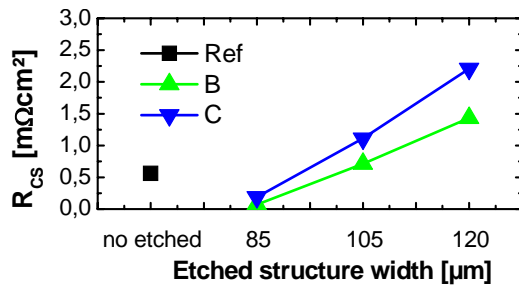


Fig. 7: Specific contact resistance R_{CS} vs. etched structure width for different pastes, determined with the transfer length method. The reference is not pre-etched. Paste A is neglected, since the values are one magnitude higher, although the same trend is observed.

The same trend turned out for the contact resistance (R_C in Ω).

Although the origin of the increasing specific contact resistance $R_{C,S}$ with increasing contact area is not clear at present, the decrease in fill factor in the *I-V* measurements can be partly explained by those results.

As possible explanation a misalignment of the printed metal structures to pre-etched structures can be excluded.

3.3 Investigating Ag island formation

Another method applied to investigate the contact mechanisms is the analysis of silver island (Ag islands) formation¹. The islands indicate the alloying process on the front side. For this investigation, the cells were treated in nitric and flouridic acid. After the paste bulk has been removed, the Ag islands can be observed. In Fig. 8 both, a draft of the analyzed area and an SEM picture are shown. The transition region of a sample that was pre-etched with a 85 μm structure followed by a 120 μm wide metal finger printing was investigated. That structure is suited for observing the Ag island formation on the one hand at the pre-etched area, and on the other hand at the with metal paste covered SiN_x . Thus, the aggressiveness against SiN_x of the metal paste can be investigated.

In Fig. 8 in the upper part (A) of the SEM picture a sufficient Ag-island formation is observable. In the middle part (B) only remaining Silver particles that were not completely removed, are indicating that the metal paste was printed in that area as well, but a fully coverage with small Ag islands can't be observed. Only next to the Ag-particles also some small Ag islands grew mainly in the valleys between the Si pyramids. This can only be explained assuming that in those valleys the SiN_x -layer thickness is smaller than on the lateral surfaces of the pyramids. Clearly to distinguish is that area where no metal paste was deposited (C). So it can be stated that, on the one hand, the contact formation process is clearly restricted to those areas that were structured by the etching process and, on the other the SiN_x layer serves as a sufficient barrier for suppressing the contact formation. The latter confirms the applicability to reduce the contact layer underneath the busbar region of solar cells and gives the chance to increase V_{OC} due to a better surface passivation.

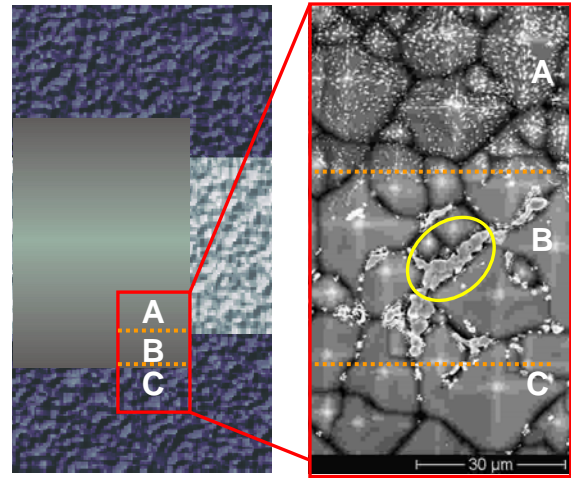


Fig. 8: Silver island formation. Draft of the structure investigated (left) including SiN_x -coated surface, pre-etched area and screen printing metallization. On the left hand side a SEM image (right) from the transition region is shown:

- A) Metal paste printed on pre-etched area, bright spots indicating Ag islands;
- B) Metal paste printed on SiN_x , remaining paste particles (yellow circle)
- C) blank SiN_x , no metal paste.

A sufficient Ag island formation is to observe in the pre-etched area, on the other hand, only Ag islands can be observed in area B in the valleys between Si pyramids.

4 CONCLUSION

The opening process using etching pastes was optimized to SiN_x films. Small finger structures with line widths of 85 μm were realized on textured surfaces. It was shown, that the ARC coating was opened completely while the Si surface was not affected by the etching process. Thus, an industrial applicable method is established, for properly structurizing dielectric layers.

Further, the silver pastes for front side metallization were optimized for the direct contact to the P-doped emitter without ARC. Metal pastes containing different types and amounts of glass frit were tested. The electrical results are very promising in terms of series resistances, where half the values compared to standard firing through process were achieved. Limited are the pre-etched structures by *FF* losses that need to be further investigated. Compared to the standard process only 0,5 % abs. lower efficiencies were obtained using a lead- and cadmium-free paste. This lead-free paste fitted the process scheme including pre-etching and cofiring best.

Further, contact resistance measurements were performed that indicated a very low achievable contact resistance for the new metallization scheme investigated. With 0,07 $\text{m}\Omega\text{cm}^2$ nearly one magnitude lower values were achieved.

By use of profound SEM investigations on Ag-island formation it was found that using an industrial SiN_x -ARC coating in combination with metal pastes that react less aggressive the contact formation process can clearly be limited to locally opened areas.

5 ACKNOWLEDGEMENTS

Ersol for processing certain test structures is gratefully acknowledged, as well as the German ministry environment and reactor safety (BMU) by funding the project ProgS (No. 0327521B).

¹ For Instance: C. Ballif, Appl. Phys. Lett. 82, No 12 (2003), pp.1878-1880,

² S. Kontermann et al., 21st EPVSEC, Dresden 2006, pp. 613-616,

³ T. Williams et al., 29th IEEE PVSC, New Orleans 2002, pp. 352-355,

⁴ M. Bähr, et al. 21st EPVSEC, Dresden 2006, pp. 859-864,

⁵ Abstract submitted by K. Neckermann et al. „Local structuring of dielectric layers on silicon for improved solar cell metallization“